Sustainable Cities and Society

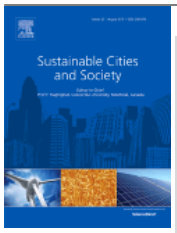

Available online at www.sciencedirect.com

ScienceDirect

Journal homepage: https://www.journals.elsevier.com/sustainable-cities-and-society/call-for-papers/special-issue-on-energy-storage-with-energy-efficient-buildi

Journal Title

ANALYSIS AND ASSESSMENT OF AN OFF-GRID SERVICE BUILDING THROUGH THE USAGE OF A DC PHOTOVOLTAIC MICROGRID

Tony Castillo C(a,b,c)*, Ana M. Macarulla(a,b), and Cruz E. Borges(a,b)

[(a)]Faculty of Engineering, University of Deusto, Bilbao, 48007, Spain
[(b)]DeustoTech - Deusto Foundation, Bilbao, 48007, Spain
[(c)]University of Oriente, Nucleus of Anzoátegui, Technological Institute, Barcelona, 6001 Venezuela

ARTICLE INFO

Article history:
Received 00 December 00
Received in revised form 00 January 00
Accepted 00 February 00

Keywords:
Off-grid building
DC-facility
PV energy
Battery performance

ABSTRACT

The aim of this paper is to present the development of an off-grid solar PV model that meets the electric consumption of a large residential building using DC. A comprehensive study has been carried out using both real consumption measurements as well as local solar irradiance and temperature levels measured in the last 30 years. Five different scenarios have been defined in which is demonstrated that the system is technically able to provide all energy needed by the facility without energy cut-off, while keeping the output rated voltage inside the tolerance values. Finally, the mean performance of the system is higher than 75 % while the losses due to the low voltage used are three times lower than the transmission losses of the AC network.

1. Introduction

Energy, in its different forms, has been used by the humanity ever since to develop new production forms. Since XX century the electricity has allowed to increase the global production while improving the quality of life. Nevertheless, as the main source of this energy are fossil fuels, not only a maintained depletion it is made, but also around 4 million of premature deaths for respiratory diseases are produced for climate change, and polluting emissions [1].

Actually, 35 % of worldwide energy is consumed in buildings [2]. For this reason, in whatever plan to reduce greenhouse gases it is of primary importance to consider them. Analysing the building consumption, it is observed that most of the home appliances, even as they are feeded with alternating current (AC) they use direct current (DC) internally leading to an AC-DC-AC conversion that a recently study has concluded to produce a 15 % of power losses [3].

On the other hand, both economical and technical barriers to install renewable energy sources are fading. Not only records in efficiency and capacity are beaten every year (see [4][5][6][7]for recent advances in different technologies of PV panels) but also its price have declined sharply: PV panels have reducing their prices from 3 USD/W to less than

* *Corresponding author.* Tel.: +34-667895980.
E-mail address: tony.castillo@opendeusto.es

Peer review under responsibility of xxxxx.

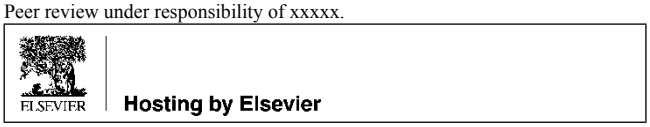

xxxx-xxxx/$ – see front matter © 2014 xxxxxxxx. Hosting by Elsevier B.V. All rights reserved.
http://dx.doi.org/10.1016/j.aebj.2014.10.012

0.49 USD/W [8] in the last 7 years; batteries have followed a similar road falling down a 35 % in the same period [9]. This is fostering the deployments of microgrids using renewable energy [10].

Nevertheless, the installation of these microgrids in buildings make a perverse effect: energy is harvested and stored in DC while then it is transformed to AC just to be rectified to DC to be finally used (or inverted another time). Namelly, in the best case a DC-AC-DC-AC cycle it is used and in the worst case (if batteries are not DC connected to the PV panels) it is needed to add a third DC-AC-DC cycle. Obviously, this increase both the losses and the costs (redundant inverters and rectifiers all along the chain).

The aim of this research is to present a methodology to size and assess the cviability of an off-grid DC photovoltaic microgrid to feed a service building with high power demand located in an urban environment. The methodology is validated using long term measurements of both load and weather data.

The rest of the paper is structured as follow. Section 2 introduces the state of the art on DC microgrids. Section 3 introduces the configuration of the microgrid presented in this paper including the sizing methodology used. Section 4 contains an explanation of the measurements and methods used in this research. Section 5 details both the results and discussion of the experiments carried. Finally, Section 6 contains the conclusions and future work.

2. Related work

There are many experiences where the advantages and disadvantages for this kind of systems have been studied. DC microgrids have been used traditionally in low power zones. For example, the Project Edison SmartDC [11] retrofitted the computer room at the University of Bath with 50 new computers that were powered by DC electricity using a central rectifier taking the electricity from the grid. After the improvement registered, a second step was to change the lighting system to a LED based illumination [12]. The entire project measures a reduction at around 30 % per a period of 18 months of experimentation.

Another place where DC grids have been used are in isolated rural areas. For example, in a rural area of India 3 residentials houses were equipped with PV panels and a battery bank on 24 V of rated output voltage. The research determines that the use of DC could reduce the energy consumption from 3.56 to 0.76 kWh [13].

In [14] a hybrid network for a residential house is studied. The scenario is composed of a set of PV panels, a wind turbine and a fuel cell that feed a circulation pump, a TV set, a fan, a portable vacuum, a fluorescent lamp, and a freezer. The results show that the usage of 12 or 24 V DC networks are safer not only for humans but also for the appliances. Moreover, it is shown that this configuration brings a reduction in cost, losses and space.

In [15] a comprehensive comparison study between AC against DC homes in 14 cities in USA have been carried out. Similar scenarios were implemented for both systems. Averaged loads were used in both cases with and without an energy storage system. Results show that DC houses have achieved a 5 % savings without the batteries and 15 % with them.

As can be seen, all research made so far covers only small residential detached houses with big roofs. Nevertheless, this is not the most typical residential buildings in several countries. For example, more than half of the population in Spain live on tower blocks in dense cities [INE] [16]. In this paper, it is presented an assessment of the viability of power up these buildings with a DC microgrid.

3. DC microgrid configuration

In this section, it is presented the main architecture of the microgrid. The test building is in Bilbao, in the north of Spain. The building provides housing for more than 300 students. It is composed of 3 towers of 10 floors each one (304 bedrooms in total), 16 living rooms, a computer room, a laundry, an industrial kitchen, and a soup kitchen. Nevertheless, some assumptions have been made:

- The kitchen will continue working with gas.
- The lift and elevator must be replaced by some DC models.
- The lights and illumination system must be replaced by [11].
- The laundry must be retrofitted with DC machines.
- The refrigeration system must be changed by its DC equivalents.
- Electronics devices and systems must be modified into a transformerless and rectifiers less in order then be able to work on DC [11].

It is expected to get important energy savings from these actions (between a 2 to a 19 % according to previous research [17][3]) but in order to be conservative with our estimations, the reductions in the load produced by these actions are not going to be taken into consideration.

The microgrid presented in this paper is loosely based on the ones presented in [18] [19]. Nevertheless, it has been improved severely by using several new control strategies for solar harvesting. In it an energy storage control of maximum and minimum State of Charge (SOC), and the use of Maximum Power Point Tracker (MPPT) has been included subsystem for increase the solar harvesting. Figure 1 shows a diagram of the microgrid used in this paper. The diagram consists of 5 subsystems:

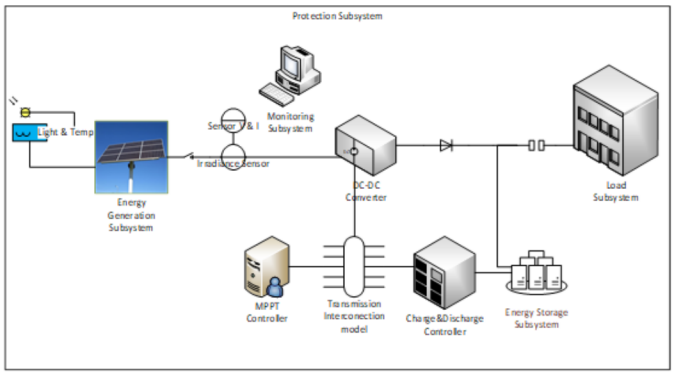

Figure 1. Microgrid diagram.

a. ***Photovoltaic generation (PV Array):***

The PV array is configured on one line in series, and 761 panels in parallel. The panel used in the simulation is the Top Sun TS6S96 [20]. It is a monocrystalline PV panel which has a performance of 16.38 %. The methodology exposed in [21] has been used to size the PV array. The key variables considered are:

- **Number of sun hours of the critical month:** 9 hours (January). January is considered the critical month not only because it has the highest consumption of the winter season but because it has the second minor irradiation level of the year. See Section 4 for a detailed discussion.
- **Energy consumption for the whole critical month:** 55505 kWh. Obtained directly from the electricity meter of the building.
- **Average consumption for a typical day of the critical month:** 1790.48 kWh. This was obtained through a k-means

analysis over the information of the critical month. See Section 4 for a detailed discussion.

- **Rated output voltage desired in solar generation stage:** 45 V. The consensus among microgrids designers is to set the panel to work near the MPPT (see Section 3-b).
- **Losses factor of the panel:** 0.8362. Taken directly from the manufacturer factsheet. Normally a losses factor of 0.8 is used [3][19].

b. Control and regulation of the MPPT (Buck converter & MPPT):

The buck control defines the operation mode of the converter DC-DC. Its function reduces the input voltage that comes from the array of PV panels to one that can be used for charge the battery bank or feed the load. The MPPT control have been sized according to [21]. The control uses an Perturb and Observe algorithm (P&O) [22] to keep the array working near to the MPPT (48.73 V) [20]. It was chosen by its simplicity and low dependency of the variables of control [23]. Also, the P&O is commercially used the most, because it only requires one voltage sensor, making this feature more attractive for its performance and low cost [24]. This control must correct the power differential (ΔP) at both, high irradiance levels and low levels that could produce a change in the MPPT goal of the system.

c. The load (Building):

The consumption was modelized as a resistive load with a variable profile that mimic the real load of the building. This load is supplied by energy storage system or by the DC-DC buck converter that regulates the power generated by the PV array. The details of the installation can be seen in [19] For convenience, all loads have been assumed to operate directly on 24 V DC.

d. Energy Storage (battery bank):

The battery bank will storage all unconsumed energy during the day to use it when the generation of energy is not high enough to keep on all the system powered on (for example at night). The battery used in the simulation is the Raylite 3MIL 25 S [25]. It is a C100 of 985 A at 25 C, 6 V battery voltage and has deep discharge technology. Batteries were sized to meet the demand of the system for 3 days following the advices from the state of the art [3][26][27][28]. The system was sized using the algorithms presented in [21]. This procedure takes into account the real percentage of energy needed by the building in days with low irradiation in order to be ahead in case of a non-typical irradiation day these include the low irradiation hours in days of good harvesting also.

To assure the longevity and the security of the batteries, it is required the use a control mechanism to reduce the degradation due to overcharge and deep discharge (DOD). For the battery used, the set points were fixed into 98.5 % and 30 % respectively. The control algorithm is based on [28]. This system cuts-off the charge of the battery bank when it gets whatever of both set points to protect the storage system against harmful levels of energy as high levels produce boiling in the electrolyte (melting the cells of the batteries) whereas low levels, even as the batteries have technology that allows deep discharges, reduce the life of the battery.

e. Wiring losses:

Due to the wiring affectation in the performance of the installation it is necessary to calculate the power losses by the conductors used or projected to be used in the system. The analysis takes as reference the distance from the top to the bottom of the building is around 30 meters. It has been assumed that all connections will have the following cables: AWG/kcmil # 1000 for main distribution among floor and AWG/kcmil # 6 to cover the "last miles" [29]. The former can handle a maximum of 455 A while the latter can support until 55 A way above the limits. To estimate the losses, it has been used just the Ohm's law.

To reduce wiring losses due to the low voltage used, it is proposed to divide the grid into 30 smaller microgrids: one per floor of the three towers as shown in figure 2.

Figure 2. Modularized microgrid for every tower.

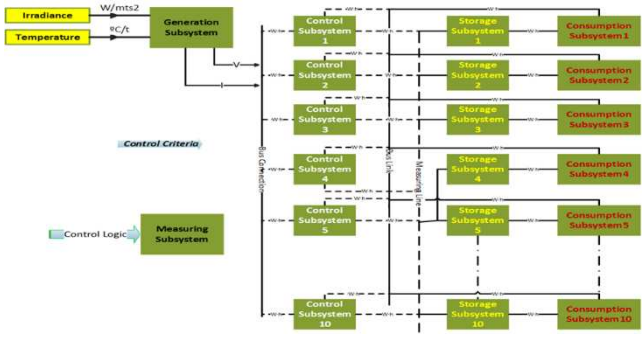

Finally, losses in protection equipment have been neglected because they are very low [17].

4. Materials and Methods

To test the behaviour of the system several scenarios have been designed covering all possible situations to which the installation will be subjected.

1. Winter typical day (WINTER): This scenario will analyze the behaviour of the system in the critical month. Namely, the one with the lowest PV generation and highest energy consumption. The next paragraph contains a detailed explanation of the methodology followed to select the critical month.
2. Summer typical day (SUMMER): This scenario is the opposite of the previous one: high PV generation due to the high irradiance level coupled with low energy consumption as during summer the occupancy descends. This scenario wanted to show that the system manages correctly excesses of energy.
3. Summer day (manipulated) (SUMMER*): This test has been built to check the behaviour of the system in an excess of solar PV generation linked with a higher consumption. This situation is not common in the test building because the occupation descends during the summer but it is the typical consumption scenario in other places of the country. We have used the energy consumption of WINTER scenario and the generation of the SUMMER scenario.
4. Lowest Irradiance for Three Consecutive Days in the Last 30 Years (LOWEST): This test check if the system could work in the worst scenario on 30 years. Moreover, this test wanted to stress the storage energy system for 72 hours. Details of how have been selected the three days can be found below.
5. Three Consecutive Days of Typical Irradiance (TYPICAL): In this test is checked the steady state of the system. To this end, we have selected the typical measurements for three consecutive days. Details of how have been selected the three days can be found below.

The Spanish Meteorological Agency (AEMET) have provided the actual irradiation and temperature data from 1986 to 2015 [30]. Primary, these data were curated eliminating wrong or inconsistent values that appeared between 26 of November to 05 of December 2010 (both included) due to a malfunctioning of the recording devices. The active power (W) have been recorded directly from the meter every 15 minutes during the years 2012 to 2014.

To select the critical month, the days with the highest power demand have been look for. It appears that the highest demand is around 62 kW. Moreover, it seems like it does not are high differences between winter and autumn/fall with respect to the power demand. Although January does not present the highest demand or the lowest irradiation, it is considered the critical month because it is the worst when considering the combination of both factors. So, the panels will be oriented to 62º which corresponds to the optimal angle for this month according to [31].

The consumption profile of the building modelled is quite stable during the year. Figure 4a shows a typical summer day, whereas in a winter typical day consumption is bigger and less stable (figure 4b). Please note that the hour in the horizontal axis is the sun hour and not the clock hour. It should be noted that the peak consumption and generation are aligned making easier to keep powered the building. The second largest peak consumption is made during the evening. In this moment, the battery bank backs up the system feeding the whole building. This pattern is only broken during long holidays and the summer term which have a flat load profile as the building is almost empty. As this is not the typical case on Spain (summer is becoming the month with the highest consumption lately in some places on Spain) the SUMMER* scenario was designed.

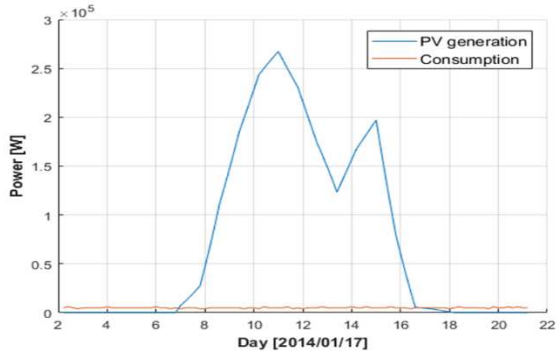

Figure 4a. Solar PV potential versus time consumption of the building in a summer day.

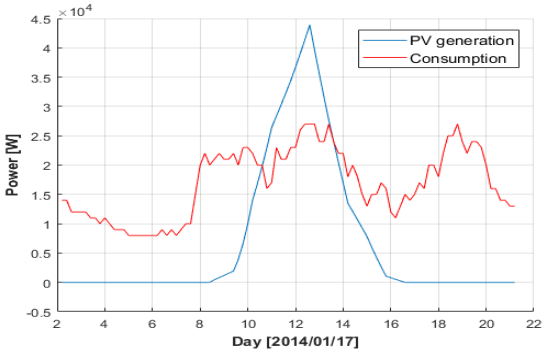

Figure 4b. Solar PV potential versus time consumption of the building in a winter day.

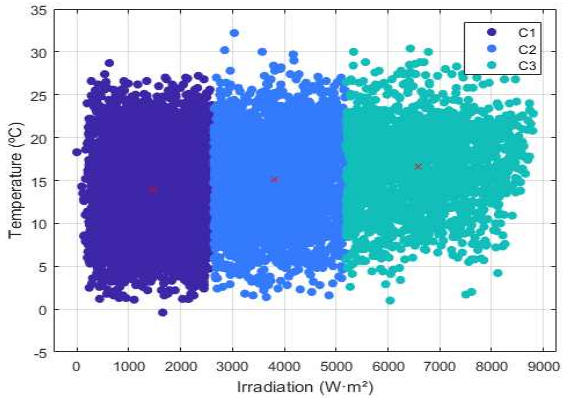

Figure 5. Solar PV behaviour after clusterization.

The information about the daily mean temperature and total irradiation were clustered using the k-means algorithm [32] with 3 groups. Figure 5 contain the result resulting clusters. As can be seen in this figure, one cluster groups the days of summer, another the winter ones and the last one the spring/autumn days together. The biggest cluster is obviously the spring/autumn one contained 47.12 %, of the data. To select the information used in the WINTER and SUMMER scenarios the day closer to the respective cluster centres have just been selected. On the same way, to select the information used in the TYPICAL scenario we have just selected the three days closer to the cluster centre of the biggest cluster. Finally, to select the information for the LOWEST scenario, the radiation of every three consecutive days have been calculated and the lowest one has been selected. Unfortunately, the historical information of the load profile is not so long. Moreover, it could not be very reasonable to use very old load profiles as the energy consumption patterns have changed a lot recently. For this reason, the load profiles have been taken on the same calendar day but of the year 2014. Please note that it has been checked that these days does not correspond to holidays, long weekends, or any similar special calendar day. As a result, the information used for every scenario were:

1. WINTER: We have selected the measurements from 2014/01/05 after applying the k-means analysis. Total energy consumption was 1.50 MWh, global irradiance was 7539.42 Wh/m^2, with a peak of 386.42 W/m^2 and an average temperature of 6.67 ºC.
2. SUMMER: We have selected the measurements from 2014/08/08 after applying the k-means analysis. Total energy consumption was only 0.789 MWh. By the other hand the irradiance and temperature increase, pushing up the generation to 1.80 MWh.
3. SUMMER*: As explained before, we have selected the energy consumption of WINTER scenario and the temperature and radiance of the SUMMER scenario.
4. LOWEST: The historical fall of irradiance levels were located during the 14, 15, and 16 of December 1999. During these days, the maximum irradiance reached 111.11 W/m^2, and the mean reached 10.95 W/m^2. The average temperature was 7.22 ^{0}C. The total energy consumption was approximately 1.32 MWh for the whole 3 days.
5. TYPICAL: The three days selected were from 18 to 21 of September 2014. During these days, the maximum irradiance reached 522.64 W/m^2, and the mean reached 91.33 W/m^2. The average temperature was 19.43 ^{0}C The total energy consumption

was 1.09 MWh. The hourly power generation of the system is near to 1.55 MWh.

In all cases, the batteries have been configured to starts with a 70 % of charge (SOC).

5. Results and discussion

The simulated experimental analysis of this work has been carried out with a desktop PC: Intel Core i5-4570, microprocessor speed 3.2 GHz, 16 GiB RAM and Windows 10 Professional 64 bits as the operating system.

Figure 6 shows the daily average energy per weeks that could have been produced for the proposed installation for 2015 and checked with the daily average consumption per weeks. As can be seen, the energy supply during the critical weeks presented in winter's months make possible to guarantee the supply of energy needed on the whole building.

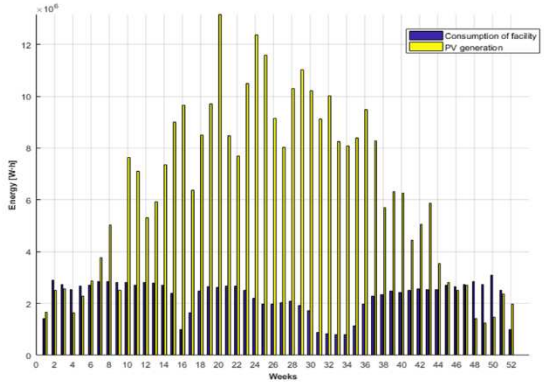

Figure 6. Solar PV potential versus consumption of the building

Figure 7 shows the results of WINTER scenario. In this figure, it could be seen that at noon the solar harvesting is higher than the consumption (red line is above the orange one) and that this excess is stored in the battery (purple line is positive). The SOC begins at 70 % (light blue curve) and slowly descends until the the sun rise and the system was capable store some energy. In this scenario, the SOC get a maximum of 70.41 % in the afternoon and finish the day with near 66.56 % so another cycle could be without huge differences.

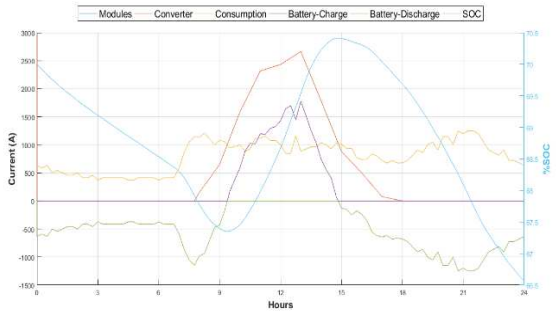

Figure 7. Currents flows & SOC present in the system for WINTER scenario.

Figure 8 shows that the voltage behaviour is very steady in this scenario staying between 22.43 and 25.99 V. The highest measurement corresponds to the hours with an excess of energy production. Finally, during the time without sun, the storage system becomes the supplier of energy of the system. This behaviour has been coded using negative values in the graph.

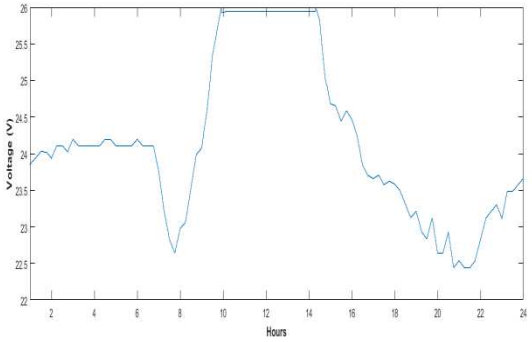

Figure 8. Supply voltage to the building in the system for WINTER scenario.

Figure 9 shows the results for the SUMMER scenario. As can be seen, the generation is much bigger that the consumption and, as a result, the SOC increases until the sun set. The final SOC is around 90 % at the end of the simulation.

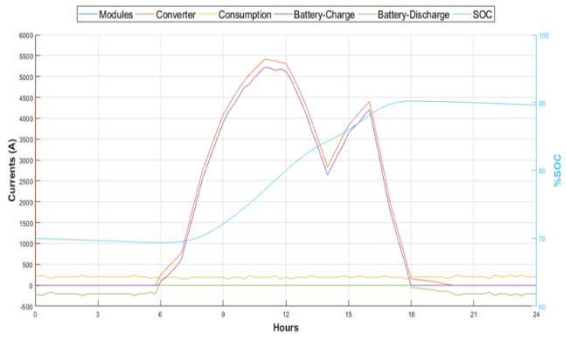

Figure 9. Currents flows & SOC present in the system for SUMMER scenario.

Figure 10 shows the voltage behaviour in this scenario. The output voltage level has a variation comprised between 24.45 and 26 V between the safe margins.

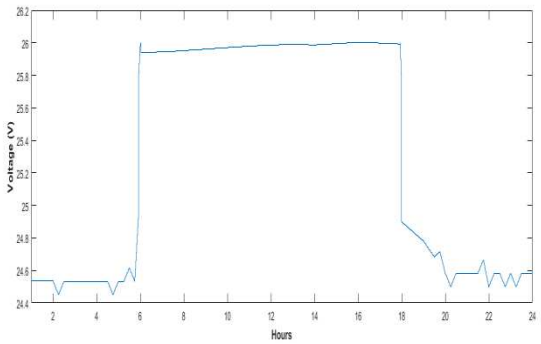

Figure 10. Supply voltage to the building in the system for SUMMER scenario.

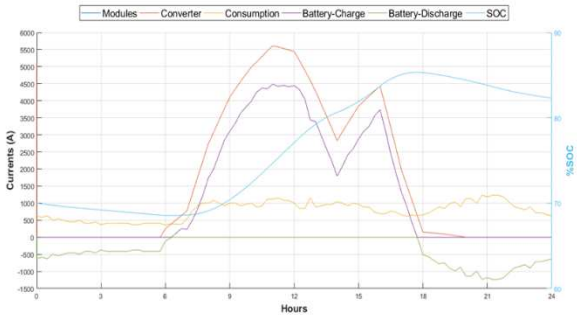

Figure 11. Currents flows & SOC present in the system for the SUMMER* scenario.

Figure 11 shows the results for the SUMMER* scenario. Even as the power demanded is significantly bigger than in the previous scenario, the PV generation is high enough for powering the system and produces an excess that is used for recharging the battery bank. In this case, the SOC achieves a maximum of 85.32 % and decreases to 83 % at the end of the simulation.

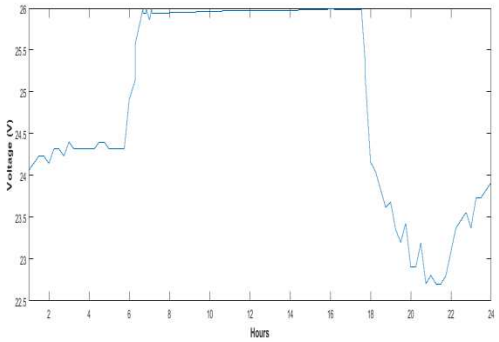

Figure 12. Supply voltage to the building in the system for SUMMER* scenario.

Figure 12 shows the voltage behaviour in this scenario. As it happened before, the output voltage level is kept between the security margins (between 22.70 to 26 V).

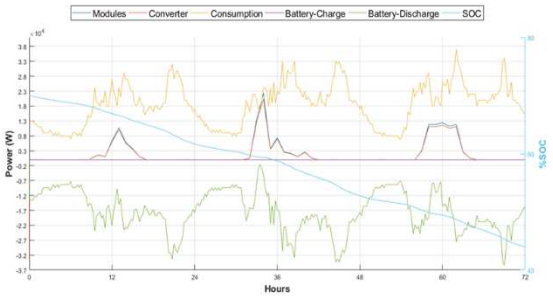

Figure 13. Power generation SOC present in the system in the LOWEST scenario.

Figure 13 shows the results for the LOWEST scenario. As can be seen, the consumption is bigger than the power generated during the entire simulation so the batteries are supplying energy constantly. Despite this complete unfavourable circumstance, the SOC in the battery bank finished at 43.95 % so the system would be able to continue operating two more days under these conditions.

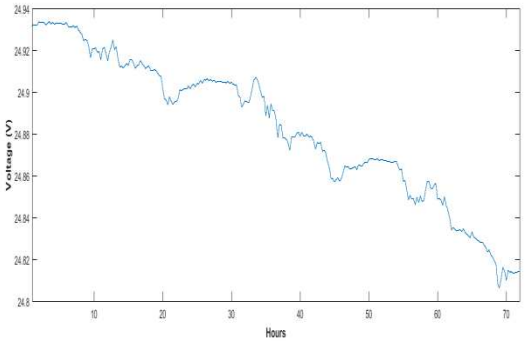

Figure 14. Supply voltage to the building in the system for LOWEST scenario.

Figure 14 shows the voltage behaviour in this scenario. In this case, as the system is continuously powered by the battery, the voltage is quite stable ranging between 24.80 to 24.93 V for the whole simulation.

Figure 15 shows the results for the TYPICAL scenario. In this scenario, we can see how the SOC varies its state periodically alternating periods of discharge (during nights) and charge (during the day). The battery bank begins at 70 % and finish at 73.51 %. So, under these conditions, the system could operate indefinitely.

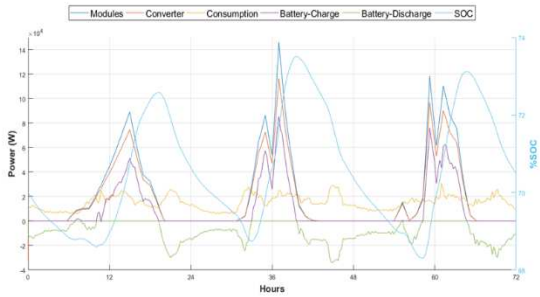

Figure 15. Power generation SOC present in the system in the TYPICAL scenario.

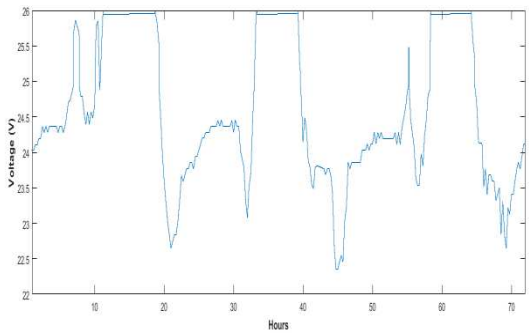

Figure 16. Supply voltage to the building in the system for TYPICAL scenario.

Figure 16 shows the voltage behaviour in this scenario. As before, the voltage is kept between 22.35 and 26 V during the entire simulation guarantee for the installation.

Finally, Table 1 presents all the efficiencies measured during the procedure of experimentation of the systems and different parts of it. Equation (1) shows the formula used to determine the different system efficiencies. In this formula, PL represents the total power consumption of the housing building (Column SYSTEM represent the performance of the entire system), PBi represents the power that is used to charge the batteries and it is extracted from the power generated in the solar harvesting (Column BUCK represents the performance of the DC-DC buck converter), PBo represents the power output-discharge prevenient of the batteries (Column BATTS represents the performance of the entire storage system) and finally, PPV represents the solar harvesting in terms of power.

$$\eta = \frac{\sum(P_L + P_{Bi} + P_{B0})}{\sum P_{PV}} * 100\% \qquad \text{eq. (1)}$$

Table 1. Efficiencies of the system.

SCENARIOS	*SYSTEM (%)*	*BUCK (%)*	*BATTS (%)*
WINTER	78.13	85.58	88.05
SUMMER	**83.78**	78.98	87.41
SUMMER*	73.51	78.45	83.52
LOWEST	56.87	**93.87**	**Inf**
TYPICAL	78.62	85.78	87.30

The efficiency of the buck converter and the batteries are in line with the ones reported by the literature [33]. The best system efficiency could be found on the SUMMER scenario with an 83.78 %, due to the consumption and the high PV generation. On the contrary, the worst system efficiency has been reached in the LOWEST scenario. In the LOWEST scenario is reached the highest buck performance 93.87 %. This result has been achieved as the system is able to manage more efficiently the usage of the energy when the generation is low. Moreover, as the energy produced is so low, the efficiency of the batteries could not be calculable. It is important to note that the TYPICAL scenario gets quite a good performance: the system reaches a 78.62 % whereas the storage system has a performance about the 87.30 % and the buck converter gets an 85.78 %. Please note that the main energetic alternatives have efficiencies around a 33 % [34].

5.1. Power losses into distribution and interconnection cabling (wiring)

Finally, the power losses due to the transmission over a low voltage will be studied. The cable will be consider as a resistance R, according to that the inductance presented in this kind of wire, the inductance is not presented in DC. Its cover is going to be ignored as is done in [17] (being R a very small resistive value for its inductive characteristic own of the electricity conductors).

As the data collected does not allow to stratify the consumption per floors, it will be assumed a uniform distribution. The peak power in the solar system is 320 kW approximately. As was mentioned before, the building is composed of 3 towers each one with 10 floors so there is a 4.44 kA/tower or 444 A/floor. This current is only reached when the panels array operates under Standard Test Conditions (STC, means temperature operation 25 ºC, irradiance of 1000 W/m2, and Air Mass 1.5) [35].

The previous calculus was simplified dividing the whole system in different stages/subsystems to reduce the power losses. The panels connection to converter produces losses of nearby 313 W while the connection among batteries and converter produces losses of nearby 313 W for all facility. The connection to the electric outlets (lights, wall plugs, security systems, etc.) produce losses nearby 12.93 kW. In sum, the whole facility would have less than 14 kW of losses in the worst scenario (3.92 %). Please note that power transmission losses in commercial networks could be as bad as 14 % [2] whereas the worldwide mean is 8.26 % [36].

6. Conclusions and future work

It is concluded that the installation can power on a medium scale building in one of the worst climate zones of Spain even in the worst conditions of the last 30 years. The system has shown to be able to maintain the voltage level between a 20 % variation. Moreover, the power losses for drop voltage and power dissipation were around a 4 % far less than the losses in transmission and distribution systems [37]. Even more, the absence of rectifiers into the home appliances could leads to bigger reduction on the conversion losses [3][17].

On the other hand, results suggest that there is an inversely proportional relation between the solar PV harvesting and the buck converter performance. For scenarios with surplus of generation, the Buck has greater losses than in scenarios where power generation did not allow large surpluses of energy.

Nevertheless, in this article have not been studied if the topological interconnection of the different components of the microgrid is optimal. Moreover, other aspects that have not been taken into consideration are the introduction of the Electric Vehicles or the covering the heating and hot water needs by using Combined Heat and Power systems or hybrids PV and Thermal solar panels.

Acknowledgements

This work was partially supported by the Erasmus Mundus SUD-UE 1301256 given by European Commission.

The authors also wanted to thank the help received from:

- Ana Gracia Scientific/Technical Project Officer of F7 Renewables and Energy Efficiency of Joint Research Centre European Commission for their help with weather (irradiance and temperature) data.
- José Luis González sub director of the hall of residence, for giving us the records of the electricity meter of the building.
- the Agencia Estatal de Meteorología (AEMET) for providing the weather information used in this this research.

REFERENCES

[1] J. L. Sawin, “Renewables 2014. Global status report,” París, 2014.

[2] K. Blok, P. Hofheinz, and J. Kerkhoven, “The 2015 energy productivity and economic prosperity index. How efficiency will drive growth, create jobs and spread wellbeing throughout society.,” 2015.

[3] O. Style, *Stand-Alone Solar Energy. Planning, sizing and installation of Stand-alone photovoltaic systems*. Middletown:

Itaca-Concern America, 2013.

[4] S. S. Shin, E. J. Yeom, W. S. Yang, S. Hur, M. G. Kim, J. Im, J. Seo, J. H. Noh, and S. Il Seok, "Colloidally prepared La-doped $BaSnO_3$ electrodes for efficient, photostable perovskite solar cells," *Science (80-.).*, vol. 356, no. 6334, pp. 167–171, Apr. 2017.

[5] M. P. Lumb, S. Mack, K. J. Schmieder, M. González, M. F. Bennett, D. Scheiman, M. Meitl, B. Fisher, S. Burroughs, K.-T. Lee, J. A. Rogers, and R. J. Walters, "GaSb-Based Solar Cells for Full Solar Spectrum Energy Harvesting," *Adv. Energy Mater.*, p. 1700345, Jul. 2017.

[6] M. Bernardi, N. Ferralis, J. H. Wan, R. Villalon, and J. C. Grossman, "Solar energy generation in three dimensions," *Energy Environ. Sci.*, vol. 5, no. 5, p. 6880, Apr. 2012.

[7] R. Crozier, "UNSW researchers set world record in solar energy efficiency | UNSW Newsroom." [Online]. Available: https://newsroom.unsw.edu.au/news/science-technology/unsw-researchers-set-world-record-solar-energy-efficiency. [Accessed: 10-Aug-2017].

[8] M. Taylor, K. Daniel, A. Ilas, and E. Young So, "Renewable Power Generation Costs IN 2014," Berlín, 2015.

[9] Kristin Seyboth, F. Sverrisson, F. Appavou, A. Brown, B. Epp, A. Leidreiter, C. Lins, E. Musolino, H. E. Murdock, K. Petrichenko, T. C. Farrell, T. T. Krader, A. Tsakiris, J. L. Sawin, J. Skeen, and B. Sovacool, "Renewables 2016 Global Status Report," 2016.

[10] N. Femia, P. Giovanni, and V. Massimo, *Power Electronics and Control Techniuqes for Maximum Energy Harvesting in Photvotltaic System*. CRC Press, Taylor & Francis Group, 2012.

[11] R. Aggarwal, M. Redfern, B. Williamson, S. Kaushik, J. Allinson, C. Janssen, C. Harris, and P. Bale, "Project Edison SmartDC – DC local network in the University Library." [Online]. Available: http://www.bath.ac.uk/ris/kta/projects/smartdc.html. [Accessed: 11-Mar-2015].

[12] B. J. Williamson, M. a. Redfern, R. K. Aggarwal, J. Allinson, C. Harris, P. Bowley, and R. Hotchkiss, "Project Edison: SMART-DC," *IEEE PES Innov. Smart Grid Technol. Conf. Eur.*, no. Lvdc, pp. 1–10, 2011.

[13] P. Sanjeev, N. P. Padhy, and P. Agarwal, "DC grid initiative in India," in *9th IFAC Symposium on Control of Power and Energy Systems (CPES)*, 2015, vol. 48, no. 30, pp. 1–6.

[14] E. Cetin, A. Yilanci, H. K. Ozturk, M. Colak, I. Kasikci, and S. Iplikci, "A micro-DC power distribution system for a residential application energized by photovoltaic-wind/fuel cell hybrid energy systems," *Energy Build.*, vol. 42, no. 8, pp. 1344–1352, 2010.

[15] V. Vossos, K. Garbesi, and H. Shen, "Energy savings from direct-DC in U.S. residential buildings," *Energy Build.*, vol. 68, no. PARTA, pp. 223–231, 2014.

[16] M. A. Casado Martín, *Comunidad de Propietarios: Las Nuevas Leyes de Propiedad Horizontal y de Multipropiedad [Condominiums: The New Laws of the Horizontal Property and Timeshare] (in Spanish)*. Madrid, 1999.

[17] D. L. Gerber, V. Vossos, W. Feng, C. Marnay, B. Nordman, and R. Brown, "A simulation-based efficiency comparison of AC and DC power distribution networks in commercial buildings," *Appl. Energy*, pp. 9–26, 2017.

[18] O. Kamara-esteban, G. Sorrosal, A. Pijoan, T. Castillo-Calzadilla, and X. Iriarte-lopez, "Bridging the Gap between Real and Simulated Environments : a Hybrid Agent-Based Smart Home Simulator Architecture for Complex Systems," in *13th IEEE International Conference on Ubiquitous Intelligence and Computing*, 2016, pp. 220–227.

[19] T. Castillo C., O. Kamara, A. Macarulla, and C. Borges, "Eco-Model for DC Electrical Systems in Standalone Buildings," in *SESDE (Simulation for Energy, Sustainable & Environment Development)*, 2016.

[20] T. Sun, "TS6S96_Mono 6 Inch 96cells." Seúl, p. 425, 2010.

[21] T. Castillo-Calzadilla, A. Macarulla, and C. Borges, "Sizing algorithms for the design of a photovoltaic facility grid-off in direct current," *IEEE Lat. Am. Trans.*, 2017.

[22] L. Liu, X. Meng, and C. Liu, "A review of maximum power point tracking methods of PV power system at uniform and partial shading," *Renew. Sustain. Energy Rev.*, vol. 53, pp. 1500–1507, 2016.

[23] M. abdul Khader aziz biabani and F. Ahmed, "Maximum power point tracking of photovoltaic panels using perturbation and observation method and fuzzy logic control based method .," in *International Conference on Electrical, Electronics, and Optimization Techniques (ICEEOT)*, 2016.

[24] L. Qin and X. Lu, "Matlab/Simulink-Based Research on Maximum Power Point Tracking of Photovoltaic Generation," in *Physics Procedia*, 2012, vol. 24, pp. 10–18.

[25] Raylite, "M-Solar Cells." Pretoria, p. 4, 1997.

[26] A. El-Ghonemy, "Photovoltaic Solar Energy: Review," *Int. J. Sci. Eng. Res.*, vol. 3, no. 11, pp. 1–43, 2012.

[27] A. Alahmed, S. I. Sidiki, Y. Alharthi, G. M. Chaudhry, and M. K. Siddiki, "Design , simulation and financial analysis of Stand-alone Photovoltaic System at University of Missouri-Kansas City , Missouri , USA," in *Photovoltaic Specialists Conference (PVSC), 2016 IEEE 43rd*, 2016, pp. 3287–3291.

[28] D. O. Akinyele, R. K. Rayudu, and N. K. C. Nair, "Development of photovoltaic power plant for remote residential applications: The socio-technical and economic perspectives," *Appl. Energy*, vol. 155, pp. 131–149, 2015.

[29] Procables, "Catálogo de Productos." General Cable, Bogotá, 2013.

[30] "Agencia Española de Metrología (AEMET)." Bilbao, 2016.

[31] The Satellite Application Facility on Climate Monitoring, "PV potential estimation utility." [Online]. Available: http://re.jrc.ec.europa.eu/pvgis/apps4/pvest.php?lang=es&map=europe. [Accessed: 16-Mar-2015].

[32] E. Sadikov, J. Madhavan, L. Wang, and A. Halevy, "Clustering query refinements by user intent," in *Proceedings of the 19th*, 2010, pp. 841–850.

[33] Ú. Ribes M., "Optimización del Diseño de Convertidorer de Potencia CC-CC," Universitat Rovira I Virgili, 2015.

[34] EIA, "Alternatives for Estimating Energy Consumption," Washington DC, 2011.

[35] A. Rezvani and M. Gandomkar, "Modeling and control of grid connected intelligent hybrid photovoltaic system using new hybrid fuzzy-neural method," *Sol. Energy*, vol. 127, pp. 1–18, 2016.

[36] World Bank, "Electric power transmission and distribution losses (% of output) | Data," 2017. [Online]. Available: http://data.worldbank.org/indicator/EG.ELC.LOSS.ZS?page=6. [Accessed: 10-Aug-2017].

[37] E. Unamuno and J. A. Barrena, "Hybrid ac/dc microgrids - Part I: Review and classification of topologies," *Renew. Sustain. Energy Rev.*, vol. 52, pp. 1251–1259, 2015.